

TRANSITION FROM FATIGUE TO IDEAL CRACKS

Hideo Kobayashi, Haruo Nakamura and Hajime Nakazawa
Tokyo Institute of Technology, Japan

INTRODUCTION

According to Elber's concept [1], the residual plastic stretch left in the wake of a steadily advancing fatigue crack interacts with the plastic zone ahead of the crack tip and causes plasticity induced crack closure above zero load. On the other hand, a saw cut crack or a fatigue pre-crack where the previous fatigue loading effect can be considered negligible compared with the following monotonic load is defined as an ideal crack. Figure 1 shows three loadings, where K_1 and K_2 are the stress intensity factors corresponding to the monotonic load and the fatigue pre-crack load, respectively; (a) is the loading for the fatigue crack ($K_1 = K_2$), (c) is the loading for the ideal crack ($K_1 \gg K_2$) and (b) is the loading between (a) and (c) ($K_1 > K_2$). As the value of K_1/K_2 increases from one to infinite, a transition from the fatigue crack to the ideal crack occurs.

It has been observed that a sudden increase in the level of loading, such as a single peak overload, for the crack under constant amplitude cyclic load has a large influence on the crack growth rate. This behavior of crack growth acceleration

and retardation has been explained on the basis of crack closure [1]. The crack growth acceleration during the single peak overload results from the transition from the fatigue crack to the ideal crack.

In this work, the comparison of the fatigue crack and

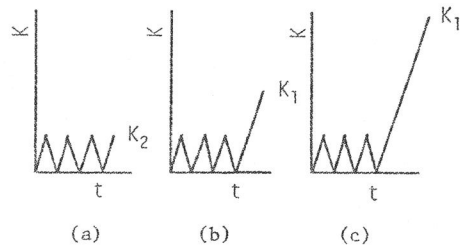


Fig. 1 Transition (b) from fatigue crack (a) to ideal crack (c).

the ideal crack is made with a special attention to plasticity induced crack closure. Using this result, a simple model to predict the transition from the fatigue crack to the ideal crack is proposed. It is shown that the model gives a fairly good prediction of acceleration.

COMPARISON OF FATIGUE AND IDEAL CRACKS

Crack extensions, Δa , on the fracture surfaces corresponding to the loadings in Fig. 1 (a), (b) and (c) could be identified fractographically as a striation, a giant striation and a sub-critical stretched zone, respectively. For the ideal crack, a relation between the sub-critical stretched zone width, SZW, and the monotonic stress intensity factor, K , or the monotonic J-integral, J , of the form

$$SZW = C_1 K^2 \quad (1)$$

in the small scale yielding (SSY) case or

$$SZW = C_1 EJ / (1 - \nu^2) \quad (2)$$

in the large scale yielding (LSY) case under plane-strain conditions has been found [2], where C_1 is a material constant, E is Young's modulus and ν is Poisson's ratio. Equation (1) or Eq. (2) presents a blunting line in the fracture toughness test. On the other hand, for the fatigue crack, a relation between the striation spacing, S , and the maximum stress intensity factor, K_{max} , of the form

$$S = C_2 K_{max}^2 \quad (3)$$

in the SSY case under the plane-strain condition has been found [3], where C_2 is a material constant for a given stress ratio, R , value.

The comparison of the fatigue crack and the ideal crack is shown in Fig. 2, where $\Delta\delta$ and δ_0 are the crack tip plastic stretches in fatigue crack growth and ideal crack growth, respectively, and $2B$ is the crack tip

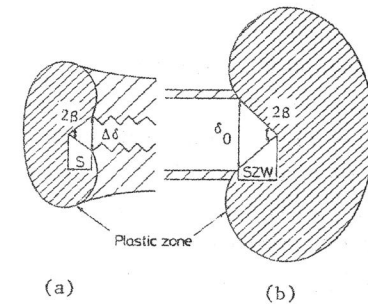
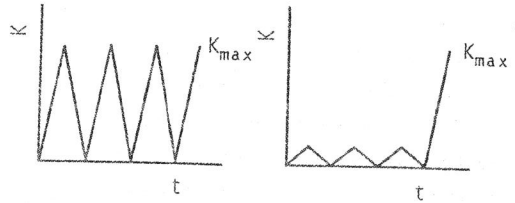


Fig. 2 Comparison of fatigue crack (a) and ideal crack (b) for a given K_{max} .

blunting angle under loading and is assumed to have a same value. On the assumption that $K = K_{max}$ for a given material, the ratio of $\Delta\delta$ to δ_0 becomes the ratio of Eq. (3) to Eq. (1) and is reduced to the following expression.

$$(\Delta\delta/\delta_0)_{K_{max}} = (S/SZW)_{K_{max}} = C_2/C_1 \quad (4)$$

The values of C_2/C_1 for alloy steels, aluminum alloys and a Ti-6Al-4V in the case that $R = 0$ become as shown in Table 1 [2, 3]. The mean values of C_2/C_1 is about 0.13.

A recent analytic study on the steadily advancing fatigue crack under the assumption of SSY according to the ideally-plastic Dugdale-Barenbratt model has shown the following result [4]

$$(\Delta\delta/\delta_0)_{K_{max}} = A[(K_{max} - K_{op})/K_{max}]^2 = A(K_{eff}/K_{max})^2 \quad (5)$$

where K_{op} is the opening stress intensity factor, K_{eff} is the effective stress intensity factor and A is about 3/4.

From Eq. (4) and Eq. (5), the values of K_{op}/K_{max} can be directly predicted as follows.

$$K_{op}/K_{max} = 1 - [(C_2/C_1)/A]^{1/2} \quad (6)$$

On the assumption that $A = 3/4$, the values of K_{op}/K_{max} for the various materials become as shown in Table 1 and show the structure-insensitive property. The mean value of K_{op}/K_{max} is about 0.58. The experimentally determined values of K_{op}/K_{max} are somewhat smaller than the predicted ones. Such differences are thought to arise mainly from ambiguity for definitions of the crack opening as well as possible experimental accuracy [3].

PREDICTION OF TRANSITION

When the single peak overload (K_1) is applied to the constant amplitude cyclic load (the maximum stress intensity factor $K_{max} = K_2$), as shown in Fig. 3 (a), K_1 can be divided into two components: K_2 for the striation for-

Table 1 Values of flow stress, σ_{fs} , C_2/C_1 and K_{op}/K_{max} for various materials.

	σ_{fs} MPa	C_2/C_1	K_{op}/K_{max}
304	496	0.11	0.62
A533B-1	588	0.12	0.60
4340	1068	0.13	0.57
10B35 (873 K)	755		
(673 K)	1362	0.09	0.64
(473 K)	1744		
Average		0.12	0.61
2017-T3	384	0.18	0.50
2024-T3	411	0.15	0.56
5083-0	217	0.20	0.49
7075-T6	537	0.20	0.48
7N01-T6	321	0.18	0.52
Average		0.18	0.52
Ti-6Al-4V	970	0.11	0.62
Total average		0.13	0.58

mation and $(K_1 - K_2)$ for the sub-critical stretched zone formation [5 ~ 8]. Then, the crack tip plastic stretch, $\Delta\delta_2 + \delta_1$, formed by the single peak overload is

$$\Delta\delta_2 + \delta_1 \propto A(K_2 - K_{op2})^2 + (K_1^2 - K_2^2) \quad (7)$$

where K_{op2} is the opening stress intensity factor.

On the other hand, the crack tip plastic stretch, $\Delta\delta_1$, formed by the constant amplitude cyclic load for the case that $K_{max} = K_1$ is

$$\Delta\delta_1 \propto A(K_1 - K_{op1})^2 \quad (8)$$

where K_{op1} is the opening stress intensity factor, as shown in Fig. 3 (b).

The ratio of Eq. (7) to Eq. (8), α , can be defined as a fatigue crack growth acceleration factor during the single peak overload for a given K_1 value and a given R value.

$$\alpha = \left(\frac{\Delta\delta_2 + \delta_1}{\Delta\delta_1} \right)_{K_1} = \frac{A(K_2 - K_{op2})^2 + (K_1^2 - K_2^2)}{A(K_1 - K_{op1})^2} \quad (9)$$

The value of K_{op}/K_{max} becomes a constant in the SSY case for a given R value.

$$K_{op}/K_{max} = K_{op1}/K_1 = K_{op2}/K_2 \quad (10)$$

Then, the value of α is given by the following expression

$$\alpha = \frac{A(1 - K_{op}/K_{max})^2 + \gamma^2 - 1}{A[(1 - K_{op}/K_{max})\gamma]^2} \quad (11)$$

where

$$\gamma = K_1/K_2 \quad (12)$$

is the overload ratio.

Equation (11) does not hold true in the LSY case and may be rewritten using Eq. (2), over a range from the SSY case to the LSY case. And it takes the form

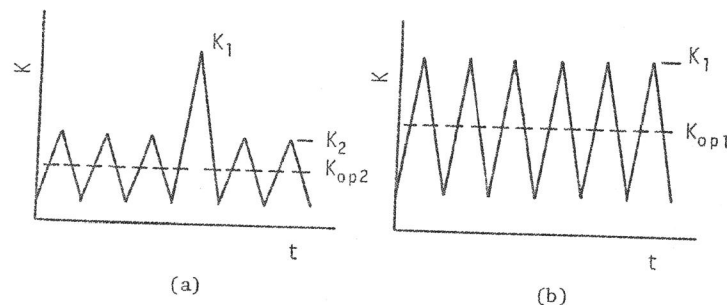


Fig. 3 Comparison of single peak overload (a) and constant amplitude cyclic load (b) for a given K_1 .

$$\alpha = \frac{(C_2/C_1)J_2 + (J_1 - J_2)}{(C_2/C_1)J_1} \quad (13)$$

where J_1 is the experimentally determined J-integral corresponding to the single peak overload and

$$J_2 = (1 - \nu^2)K_2^2/E \quad (14)$$

COMPARISON OF PREDICTIONS AND EXPERIMENTS

The value of α can be determined experimentally as the ratio of the giant striation spacing, GS, formed by the single peak overload to the striation spacing, S, formed by the constant amplitude cyclic load for a given K_1 or J_1 value and a given R value.

$$\alpha = (GS/S)_{K_1 \text{ or } J_1} \quad (15)$$

The values of $(GS/S)_{K_1}$ or $(GS/S)_{J_1}$ on two aluminum alloys, 2017-T3 and 5083-O, and a Ti-6Al-4V alloy have been examined quantitatively by the authors [8].

The comparison of predictions and experiments for the three alloys in the case that $R = 0$ is shown in Fig. 4; (a) and (b) present the results under the assumptions of SSY and LSY, respectively. Figure 5 also shows the comparison of predictions and experiments for the 2017-T3 alloy in the case that $R = 0.4$. Equation (11) and Eq. (13) give fairly good predictions for the two R values. The latter is especially useful for quantitative evaluation in the LSY case.

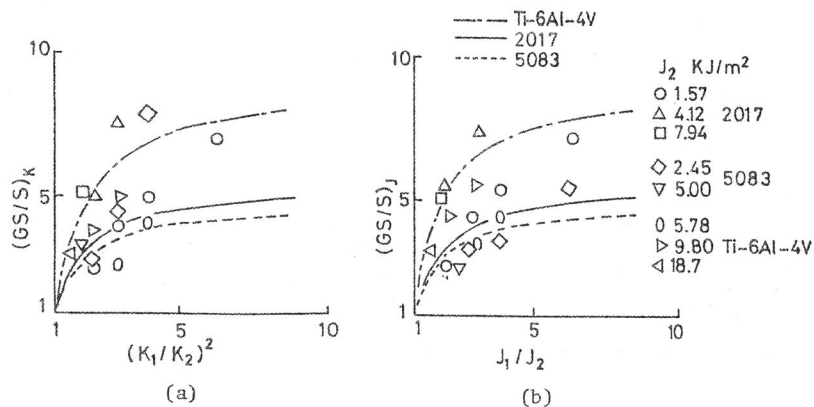


Fig. 4 Comparison of predictions (lines) and experiments (symbols) for three alloys under the assumptions of SSY (a) and LSY (b).

The fatigue pre-crack requirement in the fracture toughness test is given by the following equation [9, 10].

$$K_f < 0.6[EJ/(1 - \nu^2)]^{1/2} \quad (16)$$

where K_f is the maximum stress intensity factor at fatigue pre-cracking and can be converted into J_f by Eq. (14). Upon the substitutions of J_2 and J_1 for J_f and J , respectively, Eq. (16) becomes as follows.

$$J_1/J_2 > 2.8 \quad (17)$$

As shown by Fig. 4, Eq. (17) prescribes a reasonable range for the ideal crack from the engineering viewpoint.

CONCLUSION

The comparison of the fatigue crack and the ideal crack is made with a special attention to plasticity induced crack closure. Using this result, a simple model to predict the transition from the fatigue crack to the ideal crack is proposed. It is shown that the model gives a fairly good prediction of the crack growth acceleration during the single peak overload.

REFERENCES

- [1] Elber, W., ASTM STP 486, (1971), 230/242.
- [2] Kobayashi, H., Nakamura, H. and Nakazawa, H., Evaluation of Blunting Line and Elastic-Plastic Fracture, ASTM STP 803, (1983), in press.
- [3] Kobayashi, H., Nakamura, H. and Nakazawa, H., Mechanics of Fatigue, AMD-Vol.47, ASME, 133/150 (1981).
- [4] Budiansky, B. and Hutchinson, J.W., Trans. ASME, Ser. A, 45(1978), 267/276.
- [5] McMillan, J.C. and Pelloux, R.M., Engng. Fracture Mech., 2(1970), 81/84.
- [6] Hertzberg, R.W., Int. Journ. of Fracture, 15(1979), R69/72.
- [7] Koterazawa, R., Strength and Structure of Solid Materials, Noordhoff, 223/235 (1976).
- [8] Kobayashi, H., Nakamura, H., Hirano, A. and Nakazawa, H., Materials, Experimentation and Design in Fatigue, Westbury House, 318/327 (1981).
- [9] JSME Standard, S 001-81, (1981).
- [10] ASTM Standard, E399-81, (1981).

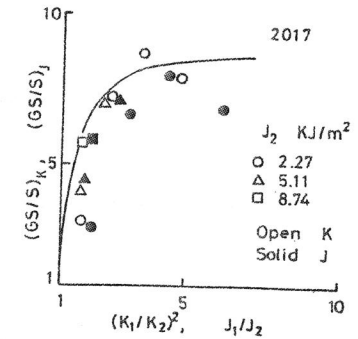


Fig. 5 Comparison of predictions (line) and experiments (symbols) for 2017-T3 in the case that $R = 0.4$.